Unsupervised Learning for Bearing Fault Identification with Vibration Data

Gianluca Nicchiotti, Idris Cherif [1] and Sebastien Kuenlin[2]

[1]*HES-SO ▪ Haute école d'ingénierie et d'architecture, Fribourg,1700, Switzerland*
gianluca.nicchiotti@hefr.ch
idris.cherif@hefr.ch

[2]*MC Monitoring, Givisiez, 1762, Switzerland*
Sebastien.Kuenlin@mc-monitoring.com

ABSTRACT

Machine learning methods are increasingly used for rotating machinery monitoring. Usually at system set up, only data of the machinery in healthy conditions, the so-called nominal data, are available for the machine learning phase. This type of training data enables fault detection capabilities and several methods such as Gaussian Mixture Model, One Class Support Vector Machines and Auto Associative Neural Networks (Autoencoders) have been already proved successful for this task.
However, in some predictive maintenance applications, information on the type of defect may represent a key element for producing actionable information, e.g. to reduce diagnostic burden and optimize spare procurement. This requires to define classification strategies based on machine learning even in absence of data representing the behaviour of the system with defects.
In this study we present an approach that uses only nominal vibration data to train an autoencoder which will enable at same time fault identification and fault classification tasks.
As faulty data are expected to possess information content which is structured differently from the healthy ones their reconstruction at output will result inaccurate. In conventional anomaly detection approaches, the module of the reconstruction error, defined as the difference between output and input, is uses to determine an unusual input such as faults.
The proposed approach represents a step forward as here a single autoencoder is used both for detection and classification.
The underlying idea is that the components of the reconstruction error vector whose module is used to trigger fault identification in classical autoencoder approaches contain the information of the fault type. This way the analysis of the different components of the reconstruction error allows to differentiate the different types of faults.
Two methods to analyse the components of the reconstruction error vector will be discussed and their respective test results will be presented
Test data have been generated with a machine fault simulator to produce 3 different types of bearing defects with different load, speed and noise conditions. A dataset of about 10000 vibration signals has been used to evaluate the classification algorithms and to benchmark them with a supervised approach.
The results obtained using the autoencoder method do not achieve the same performances as the conventional supervised learning algorithms. However, they proved to be 88% accurate in classification when SNR is above 0dB with the ranking based method overperforming the barycentre one.

1. INTRODUCTION

Diagnostics is a crucial aspect for rotating machinery maintenance. Data processing methodologies range from traditional techniques such as frequency analysis to more innovative approaches like machine learning. In diagnostics process two main steps are often distinguished: detection and identification/classification. Detection aims to recognize the presence or absence of a defect. This can be sufficient in some situations where it is simply necessary to know if a machine is functioning correctly or if it requires intervention. Nevertheless, to optimize maintenance and repair processes, it is often essential to precisely target determining which component is failing: this requires fault identification.

Data-driven approaches are progressively more employed for anomaly detection and fault classification for machine condition monitoring purposes. However, high integrity systems could not always use the supervised learning/classification process needed for fault classification.

This depends on the fact that, at machine installation time, only healthy (nominal) data are available for training. Unsupervised learning offers a solution to fault detection by modeling nominal data and using a distance measure and a threshold for determining abnormality (Samanta, Al-Balushi, & Al-Araimi, 2003; Jack & Nandi, 2002; Booth & McDonald, 1998; Sanz, Perera, & Huerta, 2007; Guttormsson, Marks, El-Sharkawi, & Kerszenbaum, 1999; Rojas & Nandi, 2006; Prego, et al., 2013; Alguindigue & Uhrig, 1991; Fulufhelo, Tshilidzi, & Unathi, 2005; Rubio & Jáuregui, 2011). However unsupervised novelty detection approaches cannot be used for fault classification.
In (Nicchiotti et al.,2016) it has been proposed a strategy to extend machine learning capabilities from fault detection to fault classification with the constraint that only nominal data are available for training. The logic is to use a priori knowledge about the effects of each fault to be classified in order to produce input training data which are somehow fault tuned. These training data are generated by computing, on nominal data, features which are known to be the most responsive to each kind of fault which has to be classified.
The approach presented in this paper represents a step forward compared to the work presented in (Nicchiotti et al.,2016), where multiple unsupervised models were trained and classification was performed by comparing the models. In this case, classification is based on the analysis of the results of a single unsupervised model.

The case study used to validate this new approach is the classification of faults in ball bearings with a machine learning approach where only healthy data are used for training. The study required taking measurements on defective bearings under various operating and noise conditions. The collected signals were preprocessed to extract training features both in time (RMS, Kurtosis, Crest Factor, etc.) and frequency domains. The frequency domain proved to be particularly effective in discriminating between different types of failures, due to the characteristic frequencies associated with the defects.

The paper is organized as follows. Next section will briefly illustrate the test rig and the data set characteristics.
A description of data-driven method used in this study will be presented in section 2. The focus will be on Auto Associative Neural Networks (AANN) .
The novel strategy to extend the data-driven capabilities from detection to classification will be described in section 4
Two methods for classifying defects will be explored: the first based on the ranking of reconstruction errors components, the second on the analysis of the barycenter of the reconstruction error when represented in a polar plot.
The results obtained with the 2 data-driven methodologies will be then compared and discussed and their robustness against noise characterized.
The classification results will be finally benchmarked against supervised approaches.

2. Acquisition Setup And Dataset

The signals were acquired using acquisition systems developed by MC-Monitoring. Measurements were conducted on a fault simulator, allowing for measurements under different operating conditions. The fault simulator enables the rotation of bearings under various load, unbalance, and speed conditions. Bearings can be affected by defects in the inner race, outer race, balls, and a case presenting a combination of defects. The defective bearings were placed at location 5 (see figure 1), and the measurement via the accelerometer is carried out along the x and y axes. The sampling rate was 50 kHz

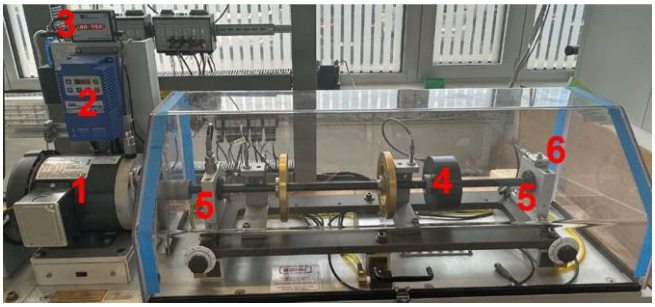

Figure 1. Machine Fault Simulator and acquisition setup. 1 AC Motor, 2 Frequency Converter ,3 Tachometer, 4 Additional mass load, 5 Right and left bearing 6Acceleration sensor x-y, 100mV/g.

For each type of bearing fault and under different loads and speed conditions, a 6-minute acquisition of the vibration signal has been performed.

After digital conversion, the raw signal undergoes filtering to remove the DC component. We then calculate the Root Mean Square (RMS) value of the filtered signal, which becomes the reference point for adding white noise. To assess the process's robustness, seven levels of white noise were added to each original signal. This resulted in a total of 140 sequences, each containing 6 minutes of healthy and faulty signal data under different load, speed, and signal-to-noise ratio (SNR) conditions.

3. Machine Learning Methods

Machine learning offers diverse tools for monitoring machine health, including density methods (KNN), boundary methods (SVM), and reconstruction methods (AANN) (Johannes, 2001). These techniques have been successfully applied to fault detection (Samanta et al., 2003; Jack & Nandi, 2002; Booth & McDonald, 1998). When used for classification, these approaches all require pre-existing fault data for training (Alguindigue & Uhrig, 1991; Fulufhelo et al., 2005; Wang et al., 2020; Prego et al., 2013).

However, acquiring such data poses a challenge when dealing with new equipment. In such scenarios, data-driven anomaly detection emerges as the only possible alternative which is

exemplified in studies by Rubio & Jáuregui (2011), Guttormsson et al. (1999), and Sanz et al. (2007) . Methods like Auto-Associative Neural Networks (Sanz et al., 2007) and one class SVM (Guttormsson et al., 1999) are among the most widely used methodologies that rely on "one-class classification", when only healthy data is available for training.

Despite their success in fault detection, one-class classification methods haven't been explored for fault identification. This research aims to bridge that gap by incorporating expert knowledge ("a priori") into these data-driven ("a posteriori") techniques, implementing fault classification within the AANN framework.

3.1. AANN

Auto-Associative Neural Networks (AANNs), also known as Replicator Neural Networks or Autoencoders, are like smart copycats in the world of artificial intelligence. These networks are trained to mimic whatever data they're given, but with a twist: they have a hidden layer with fewer neurons than the input and output. This "bottleneck", shown in Figure 1, forces them to compress the information, essentially learning the key features of the data they're trained on.

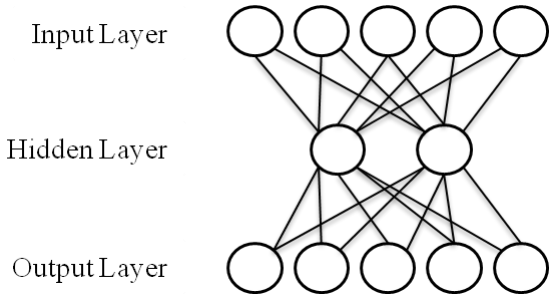

Figure 2. AANN Architecture.

Imagine training an AANN with healthy equipment data. Once trained, it can accurately reproduce similar healthy data. However, faulty data will contain different patterns that the AANN struggles to compress in the bottleneck. This results in a larger reconstruction error, which is the difference between the original data and the AANN's attempt to recreate it.

The reconstruction error can be considered as a measure of strangeness. The higher the error, the more different the data is from what the AANN knows as "healthy." By setting a threshold for this error, we can create a simple fault detection system: anything with an error above the threshold is likely faulty.

In practice once a new sample is processed by the AANN, the measure of the difference between output and input vectors, the Reconstruction Error (RE) of an input vector X, is computed as

$$RE = \|X - O_X\| \quad (1)$$

where O_X is the output of the AANN and || symbol stands for any p-norm. Once computed the R_E, a fault or anomaly detection logic can be easily implemented for instance by thresholding.

4. FAULT IDENTIFICATION STRATEGY

This section aims to examine the usage the reconstruction error of an autoencoder to classify different types of defects.

To compensate for the lack signals associated with the defects, the idea is to leverage the "a priori" knowledge of the phenomena linked to the type of fault and encode it within the autoencoder process. As shown in figure 3, this process requires an initial step consisting of extracting features from the signal through appropriate signal processing techniques.

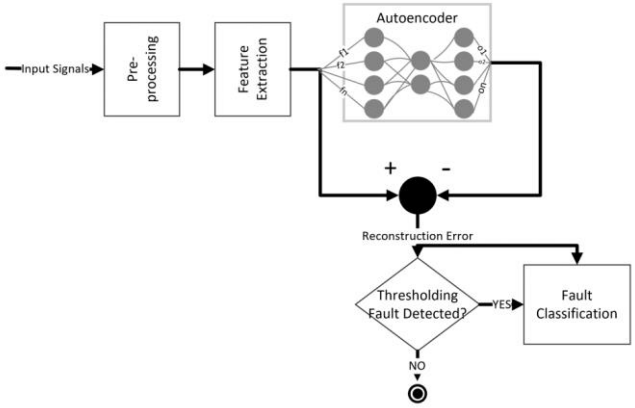

Figure 3. Main Processing Steps.

4.1. Pre-processing

In the subsequent discussion, the term "feature" refers to an individual measurable attribute of the observed phenomenon. In this research, the features represent various characteristics of the signals extractable from the signals. Features represent unique clues about a machine's condition, like symptoms for a doctor. Think of these features as different dials on a dashboard, each showing a different aspect of the machine's health.

Raw sensor data from ball bearings needs preparation before computing features and feeding it into machine learning algorithms. This involves filtering, windowing, and extracting the signal's "envelope".

- Filtering - Since the information we care about lies above 2 kHz, lower frequencies are irrelevant and clutter the analysis. We utilize a Butterworth bandpass filter [2-22kHz]to selectively remove them. In this proof of concept, we decided to use such a large bandwidth to represent the worst case. Practically, it is more efficient to filter around the frequency resonance of the entire system (motor, bearing, sensors, etc..) which is between generally somewhere between 2kHz and 20kHz to minimize the noise. However, as we wanted a "generic" system, we decided to use the overall bandwidth of our acquisition system. This also presents a practical benefit of not requiring to configure the filter during the installation procedure.

- Envelope Extraction - Ball bearing vibrations, like the one shown in Figure 3, contain information in their "envelope". This envelope reflects the modulation of the bearing's natural resonance frequency caused by impacts between rolling elements and defects. To uncover the characteristic frequencies of these defects, we calculate the Fast Fourier Transform (FFT) on the extracted envelope, not the raw signal. As most of the rotating machines we monitor in our applications run between 25Hz and 60Hz, we know that the characteristic frequency of the faults (BPFO, BPFI, etc) are between, let say, 5Hz an 500Hz, so the envelope size was chosen according to these values.

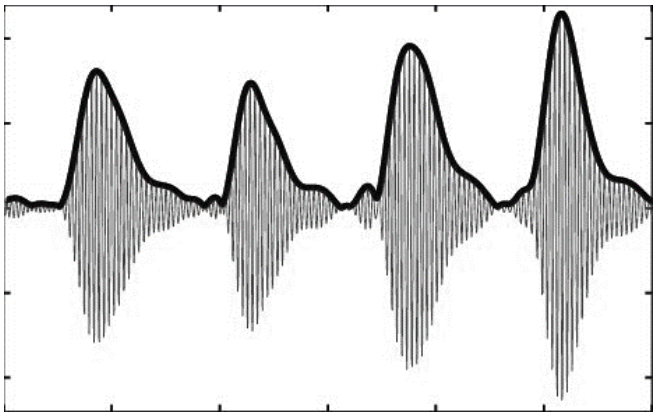

Figure 4. Bearing signal: Raw (slim lines) Envelope (bold lines)

- Windowing - To enhance the accuracy of frequency analysis, we apply a Hann window to the filtered data. This window smooths the signal edges, reducing artifacts in the resulting spectrum. The measured signal (240 s) will be divided into 1-second samples with a 1/2-second overlap. The choice of 1 second allows balancing the need for enough signals for machine learning model training and retaining sufficient characteristic information of the vibrational signal generated by the bearing. A too small window would make the model unreliable if the pseudo-periodic nature of the signal is not preserved in the sample. A too large window would also not allow good model generalization due to the more limited training dataset.

4.2. Feature extraction

Features have been extracted with time domain and frequency domain analysis.

In the time domain, signals from defective bearings exhibit periodic impulses corresponding to impacts between the balls and the cage defect or between the defective ball and the metallic components. The impulses excite the resonance frequencies of the system. Each impact can be compared to the impulse response of the system due to the short duration of contact between a ball and the defect The presence of defects in a machine can be detected by analysing the vibration signal. Defects increase the energy of the vibration signal and modify its statistical distribution. These changes can be used to identify the presence and severity of the defects. Time domain features used in this study are (Hornavar & Martin, 1995): RMS,Crest Factor, Kurtosis, Skewness, Impulse Factor and Form Factor.

Each bearing has a unique "fingerprint", its characteristic frequencies, determined by its geometry and rotation speed. (Kamaras et al. ,1995, Andhare, 2010)

- FTF - Fundamental Train Frequency: This is the rotation frequency of the bearing cage.

- BPFI - Ball Pass Frequency of the Inner Race: This frequency is generated by the passage of balls over the inner ring.

- BPFO - Ball Pass Frequency of the Outer Race: This frequency is generated by the passage of balls over the outer ring.

- BSF - Ball Spin Frequency: This frequency is related to the rotation of the balls.

When a fault develops, these specific frequencies become amplified, acting like warning lights. These frequencies not only reveal the presence of a problem but also pinpoint the exact type of fault, allowing for targeted repairs and preventing unnecessary downtime. Hence to identify faults in bearings, features were extracted from the vibration signal's envelope spectrum. These features included the peak ratio amplitudes of characteristic frequencies related to bearing health: the Ball Pass Frequency Outer Race (BPFO), Ball Pass Frequency Inner Race (BPFI), and Ball Spin Frequency (BSF). Additionally, the spectral centroid and the energy in the band 10-20 kHz were included. These features formed the frequency "fingerprint" of the bearing's health and were fed into an Auto Associative Neural Network (AANN) for fault classification.

To extract the features, we first chopped the time signal into half second intervals, making sure to overlap them by 0.25s to capture any important transitions. From each chunk, we

then extracted 14 specific features which we fed into the autoencoder for further analysis.

4.3. Classification

The fault detection by autoencoder is based on the premise that the reconstruction error for data similar to those used for training will be lower than the error for data from faulty bearings.

Since different features do not all have the same range of values, the data has to be standardized (Equation 2). Each new set of tested data will be standardized using the mean and standard deviation of the training data.

$$F_i = \frac{f_i - \mu_i}{\sigma_i} \qquad (2)$$

Where f_i is the value to be standardized, μ_i , σ_i are the mean and the standard deviation of the training set for feature i and F_i is the standardized feature value.

The parameters of the autoencoder have been determined according to the average reconstruction error on healthy data. The autoencoder has a single hidden layer which contain 10 neurons This value represents a good compromise between low reconstruction error and moderate training time. The maximum number of iterations (Epochs) for training is set to 500 beyond this, the improvement in performance is not significant.

For each feature F_i at the input, the autoencoder calculates a corresponding output O_i . The difference $E_i = \|F_i - O_i\|$ represents the components of the reconstruction error along the various axes represented by the features used, as shown in Figure 5.

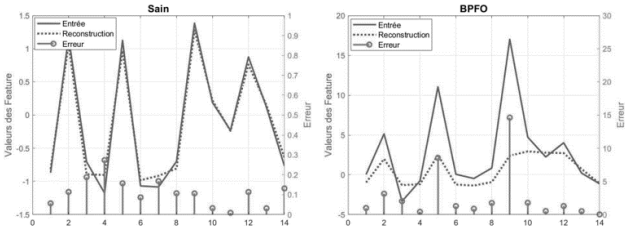

Figure 5: Reconstruction error for a healthy signal (left) and outer race fault (right). X-axis represent the feature index Errors E_i in stems (vertical lines), continuous lines input features dotted features as reconstructed by autoencoder

The two classification strategies here presented assume that the relative values of components E_i of the reconstruction error depend on the type of defect.

The first approach maps E_i on a polar plot (Figure 6), and uses the angle of the reconstruction error to discriminate the different types of faults.

To differentiate between fault types, each feature i is assigned a specific angle (θ_i). Using a priori knowledge about fault behavior, these angles are carefully chosen to maximize the angular separation between features clearly associated with different faults (e.g., Inner Race, Outer Race, Ball). For example, BPFO, BPFI, and BSF might be assigned 0°, 120°, and 240° directions, respectively.

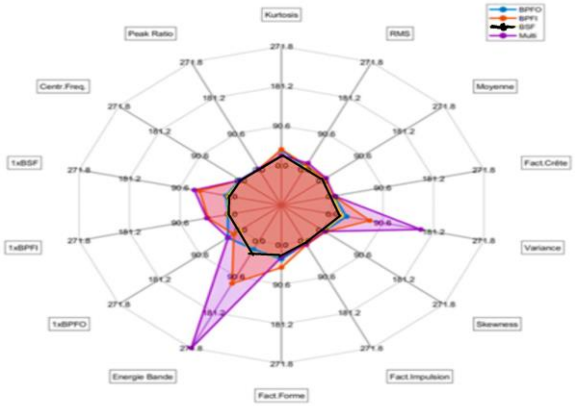

Figure 6: Polar Plot of the reconstruction error. Blue contour represents the shape of outer race fault, Red of inner race, Black ball fault, Violet Multiple faults. Different faults types correspond to different contours.

Next, each feature's reconstruction error component E_i is represented as a 2D vector $\overrightarrow{E_i}$ where the magnitude reflects the error value of the component itself and the angle corresponds to the pre-assigned θ_i based on fault type a priori knowledge. By summing these vectors, a resulting reconstruction vector $\vec{V}$ is created

$$\vec{V} = \sum_{i=1}^{N} \overrightarrow{E_i} \qquad (3)$$

Based on the vector direction Θ of $\vec{V}$ $with$ Θ=arg($\vec{V}$) the fault type can be classified.

For instance, if Θ is falling within -60° to 60° we can classify the fault as inner race between 60° and 180° as outer race, else as ball error. The underlying idea is that reconstruction errors not strictly dependent on the type of defect interfere destructively, highlighting the direction of the defect in the polar plot.

The second method assumes different fault types make it harder for the autoencoder to reconstruct certain feature components. By leveraging a priori knowledge, we anticipate the ranking of reconstruction errors magnitude for the features across different fault scenarios as shown in Table 1.

Table 1. Ranking fault signatures

Fault type	Reconstruction error $E_i = \|F_i - O_i\|$													
	←Bigger												Smaller →	
Inner	1	8	10	5	9	12	7	2	11	6	3	4	13	14
Outer	9	5	12	8	11	1	10	2	7	6	3	4	13	14
Ball	12	8	1	5	9	7	6	10	11	2	3	4	13	14

This expected ranking serves as a signature to identify the actual fault based on the observed ranking of reconstruction errors. Comparing the actual observed order to the expected ranking enables the classification task.

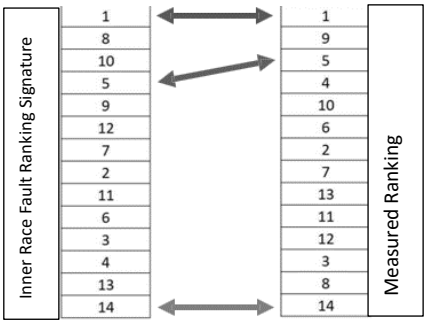

Figure 7: Example of ranking signature for Outer Race Fault and RBO algorithm

To effectively compare ranking list and classify the fault type, the algorithm needs to consider the varying importance of features in their ranked order (see Figure 7). The correspondence between two top-ranked features (top arrow) is more important than two lower-ranked features (bottom arrow). Additionally, two identical features that are not at the same rank (center arrow) must be taken into account. To accomplish this, the Rank Biased Overlap (RBO) algorithm (Joshi 2021), which meets these requirements, was used to compare the rankings. This algorithm allows assigning a weight (p) more or less significant to elements at the top of the ranking. The result of the comparison between the two lists is a number between 0 and 1 (the value '1' is obtained for two identical lists).

5. TEST RESULTS

An autoencoder with 14 input features and a single hidden layer with 8 nodes to distinguish healthy and faulty system states has been trained with 3000 healthy samples, each represented by a vector of 14 features extracted from a 0.25-second signal window. The model's performance was evaluated on 3000 healthy and 9000 faulty samples. While confusion matrices provided insights into classification errors, this document focuses on precision, defined as the ratio of the total number of correct predictions to the total number of predictions made by the model.

Figure 8 demonstrates the model's ability to accurately detect healthy states with excellent precision even when dealing with high levels of noise in the signal.

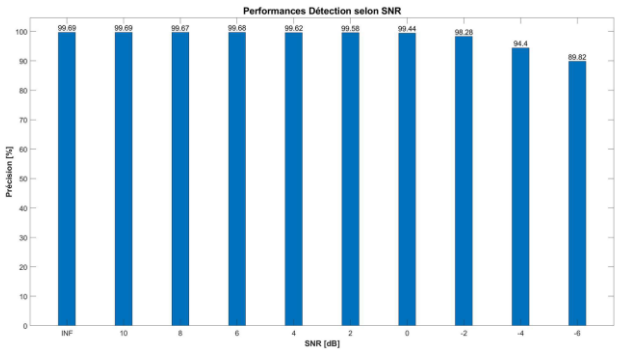

Figure 8: Precision of the anomaly detection as a function of SNR(dB)

To detecting faults, we set a threshold (Th_D) based on the reconstruction error (RE). If RE exceeds Th_D, a fault is likely present. This threshold is calculated as the mean (μ_{TS}) plus three times the standard deviation (σ_{TS}) of the reconstruction error computed on the training data (Equation 4).

$$Th_D = \mu_{TS} + 3 \cdot \sigma_{TS} \quad (4)$$

The autoencoder demonstrates exceptional anomaly detection capabilities even under low noise conditions, achieving precision levels exceeding 99.4% for signal-to-noise ratios (SNR) up to 0 dB. However, as noise levels increase, performance drops and false alarms become a concern, at SNR 6 dB, precision falls below 90%.

5.1. Vector Direction classification

Initially, with 14 features, the method based on the direction of the reconstruction vector (Θ=arg($\vec{V}$)) only achieved a 76.8% precision. The unsatisfactory percentage is likely due to the correlation between some features which produced the same interference pattern. Therefore, we applied Principal Component Analysis (PCA) (Shlens, 2014) to identify redundancies and reduce the number of features to 8 This process ends up with the selection of the most informative features, in statistical sense, like RMS, Kurtosis, Peak Factor, Impulse Factor, and key frequency components). This dimensionality reduction significantly improved classification performance, boosting the precision to 87.94%.

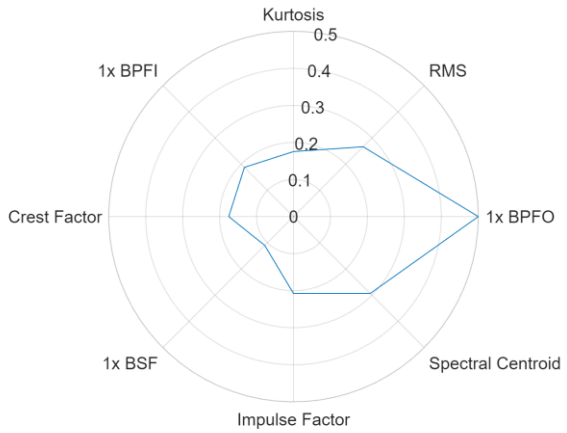

Figure 9: Polar Plot with 8 features pour outer race fault

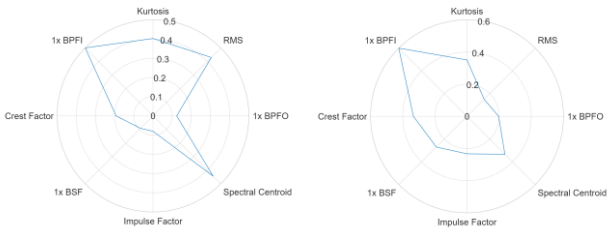

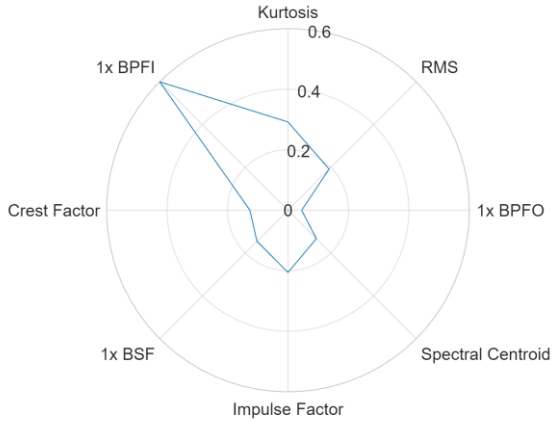

Figure 10: Polar Plots with 8 features for an inner race fault

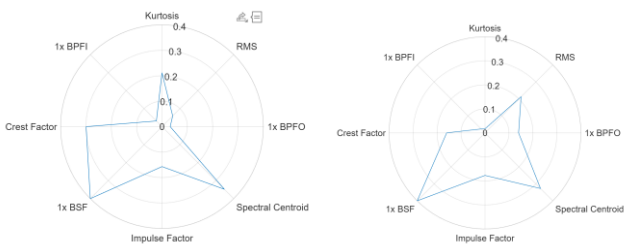

Figure 11: Polar Plots with 8 features for a ball fault

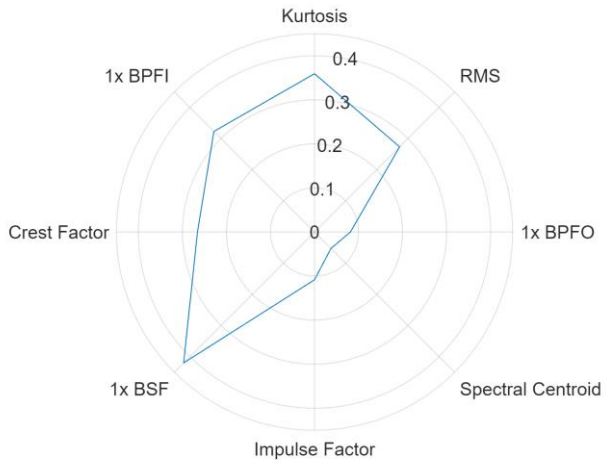

Figure 12: Polar Plots with 8 features for a ball fault, with misclassification

In addition to automated fault classification, our method provides a visual tool for identifying different fault types. Figures 9-11 showcase polar diagrams where each plot displays examples correctly classified. Figure 12, however, depicts a scenario where misclassification occurred.

In some maintenance situations, where misidentifying a failure could have serious consequences, operators can leverage these visualizations to perform a semi-automated diagnosis, especially if the automated results lack sufficient confidence. This allows them to combine the model's insights with their own expertise for a more informed decision.

5.2. Rank Order classification

When using the rank order RBO method for classification, the initial precision with 14 features was only 41.46%. Similar to the previous approach, we reduced the number of features to decrease redundancy and eliminate less relevant information. Using the same features as the "vector direction" classifier, the RBO method improved, and achieved a maximum precision of 76.8% when the parameter p (Joshi 2021) is set to p =0.9. The parameter p determines the weighting of the first positions in the similarity measurement between two ranked lists. By adjusting the value of p, it is possible to control the importance given to the first positions compared to the subsequent positions, thus providing flexibility to evaluate the similarity between ranked lists according to different criteria. The value of p is chosen between 0 and 1. In this case, it has been decided to give more importance to the first positions in the ranking, which have a more significant impact on the classification performances.

Therefore, the « directional » classifier appears more effective in our tests.

While unsupervised methods like RBO offer an advantage in not requiring labelled data, their precision in this case

(76.8%) falls short compared to supervised learning (>99% precision). (Cherif, 2023) This is likely due to the inclusion of actual fault data in the training set for supervised methods, providing them with a more direct understanding of failure patterns.

6. CONCLUSIONS

The application of unsupervised machine learning techniques for detecting bearing faults and anomalies in rotating machinery offers a compelling array of advantages for practical business implementations. By eliminating the need for labeled faulty data, these approaches streamline the deployment process, making it more accessible and cost-effective for industrial settings.

The ability to operate without pre-existing fault data enables unsupervised algorithms to uncover previously unrecognized patterns and anomalies, providing early detection of faults and proactive maintenance opportunities. This early detection capability, coupled with scalability and adaptability to changing conditions, empowers businesses to enhance reliability, minimize downtime, and optimize maintenance strategies.

In essence, leveraging unsupervised machine learning in industrial contexts not only circumvents the challenges associated with acquiring labeled data but also delivers tangible benefits in terms of reliability, efficiency, and cost-effectiveness. This approach represents a transformative paradigm for bearing fault detection and anomaly monitoring, enabling businesses to proactively manage their assets and maximize operational performance without relying on historical fault data.

However, whilst supervised and unsupervised methods show similar performance in defect detection, our proposed approach using an autoencoder for classification falls short compared to supervised learning. However, our method offers the crucial advantage of not needing rare defect data for training. This combination of unsupervised anomaly detection and classification enables defect detection without labeled data.

The "directional error" method achieves a promising 87.94% accuracy through optimized feature selection.

To further improve our classification system, we are pursuing two complementary research directions:

1. Improving precision over time: We're exploring how to combine classification results over time to potentially boost precision.
2. Implementing a rejection logic (Bartlett & WegKamp, 2008; Chow ,1970): This framework aims to prevent critical misclassifications by allowing the model to avoid predictions when uncertain, at a predefined cost. This enables semi-automatic diagnostics where polar plots of ambiguous cases can be sent to operators for confirmation.

From the validation point of view, it has been planned to validate our methodology on HUST bearing dataset (https://data.mendeley.com/datasets/cbv7jyx4p9/3)

NOMENCLATURE

E_i	Reconstruction error component
Θ	Direction of Reconstruction Vector
p	Weight of RBO
RE	Reconstruction Error
Th_D	Detection Threshold
$\vec{V}$	Reconstruction vector

REFERENCES

Alguindigue, I., & Uhrig, R. E. (1991). Vibration monitoring with artificial neural networks. *Tennessee: OECD publishing.*

Andhare, A. (2010). Condition Monitoring of Rolling Element Bearings. *Lap Lambert Academic Publishing GmbH KG*. p.9-11, 65-72.

Bartlett P. L. and Wegkamp M. H. (2008) Classification with a reject option using a hinge loss. *Journal of Machine Learning Research, 9:*1823–1840, 2008.

Bilmes, J. A. (1998). A Gentle Tutorial of the EM Algorithm and its Application to Parameter Estimation for Gaussian Mixture and Hidden Markov Models. *Berkeley: International computer science institute.*

Bishop, C. M. (2006). Pattern Recognition and Machine Learning. *New York: Springer Science+Business Media.*

Booth, C., & McDonald, J. R. (1998). The use of artificial neural networks for condition monitoring of electrical power transformers. *Neurocomputing, 97-109.*

Cherif I. (2023) Détection des défauts de roulements par analyse de vibrations. *Travail de Bachelor Haute école d'ingénierie et d'architecture, Fribourg*

Chow. C. K. (1970) On optimum recognition error and reject tradeoff. *IEEE Transactions on Information Theory*, 16(1):41–46, 1970.

Fulufhelo, V. N., Tshilidzi, M., & Unathi, M. (2005). Early classifications of bearing faults using hidden Markov models, Gaussian mixture models, Mel- frequency cepstral coefficients and fractals. *International Journal of Innovative Computing, Information and Control*, 1281-1299.

Guttormsson, S., Marks, R., El-Sharkawi, M., & Kerszenbaum, I. (1999). Elliptical novelty grouping for on-line short-turn detection of excited running rotors. *Energy Conversion, IEEE Transactions on*, 16-22.

Honarvar, F. and Martin, H.R. (1995) Application of statistical moments to bearing fault detection. *Applied acoustics*, 44 : p.67-78,

Jack, L. B., & Nandi, A. K. (2002). Fault detection using support vector machines and artificial neural networks, augmented by genetic algorithms. *Mechanical Systems and Signal Processing*, 373-390.

Johannes, M. D. (2001). One-class classification. *Delft: Advanced School for Computing and Imaging*.

Joshi, P. "RBO v/s Kendall Tau to compare ranked lists of items". Towards Data Science. *Retrieved 23-01-2024.: https://towardsdatascience.com/rbo-v-s-kendall-tau-to- compare-ranked-lists-of-items-8776c5182899*

Kramer, M. A. (1992). Autoassociative neural networks. *Computers & chemical engineering*, 16(4), 313-328.

Kamaras, K., Garantziotis, A., & Dimitrakopoulos, I. Vibration Analysis of Rolling Element Bearings (Air Conditioning Motor Case Study). *Retrieved January 25, 2023 https: //fnt.com.cy/ images/ Rolling%20Element%20Bearings%20Vibration %20Analysis.pdf*

Nicchiotti, G., Fromaigeat, L., & Etienne, L. (2016). "Machine Learning Strategy for Fault Classification Using Only Nominal Data". *PHME Conference 2016*

Ng, A. (2015, September 21). Machine Learning Course Materials. *Retrieved January 15, 2023, from http://cs229.stanford.edu/materials.html*

Prego, T. d., de Lima, A. A., Netto, S. L., da Silva, E.A., Gutierrez, R. H., Monteiro, U. A.,Vaz, L. (2013). On Fault Classification in Rotating Machines using Fourier Domain Features and Neural Networks. *Circuits and Systems (LASCAS), 2013 IEEE Fourth Latin American Symposium n*, 1-4.

Rojas, A., & Nandi, A. K. (2006). Practical scheme for fast detection and classification of rolling-element bearing faults using support vector machines. *Mechanical Systems and Signal Processing 20*, 1523-1536.

Rubio, E., & Jáuregui, J. C. (2011). Time-Frequency Analysis for Rotor-Rubbing Diagnosis. In F. Ebrahimi, *Advances in Vibration Analysis Research* (pp. ISBN: 978-953-307-209-8, InTech, DOI:10.5772/15186).

Samanta, B., Al-Balushi, K. R., & Al-Araimi, S. A. (2003). Artificial neural networks and support vector machines with genetix algorithm for bearing fault detection. *Engineering Applications of Artificial Intelligence*, 657-665.

Sanz, J., Perera, R., & Huerta, C. (2007). Fault diagnosis of rotating machinery based on auto-associative neural networks and wavelet transforms. *Journal of Sound and Vibration 302*, 981-999.

Shlens, J. (2014). A tutorial on principal component analysis. Retrieved 14.2.2024 *https://doi.org/10.48550/arXiv.1404.1100*

Schölkopf, B., Platt, J. C., Shawe-Taylor, J., & Smola, A. J. (2001). Estimating the Support of a High-Dimensional Distribution. *Neural Computation, 13*(7), 1443-1471.

BIOGRAPHIES

Gianluca Nicchiotti received an MSc in Physics from Università di Genova, Italy in 1987 and an MSc in Applied Science from Cranfield University UK in 2013. Since 2022 he holds the chair of Signal Processing at Haute école d'ingénierie et d'architecture in Fribourg. From 2005 to 2022 worked in the aerospace domain as system engineer by Meggitt, Switzerland. Prior to Meggitt, he managed an image processing research team at Elba Research Center and developed algorithms for sport video special effects at Dartfish. His career started at Elsag Bailey R&D in underwater acoustic cameras field. He is author of more than 50 papers and 5 patents. His current research interests are quantum computing and machine learning.

Idris Cherif got a degree in Electronic Engineering from Haute école d'ingénierie et d'architecture in Fribourg now he is R&D engineer at Inergio.

Sebastian Kuenlin's received a degree in Electronic Engineering from Haute école d'ingénierie et d'architecture in Fribourg, Switzerland, where he earned a Bachelor of Science HES in Electrical Engineering with a specialization in Electronics in 2010. At the end of his studies, he conducted his diploma work at Lawrence Berkeley National Laboratory, focusing on testing stave/module systems for the ATLAS detector at CERN. During this time, he developed an electronic test bench based on FPGA. Transitioning to MC-monitoring SA in 2011, Sébastien worked in embedded system development before assuming leadership roles, ultimately becoming Chief Technology Officer and of MC-monitoring SA in 2018. His current areas of expertise are acquisition system and signal processing.